The Journal of Immunology

IFN-γ–Producing CD4$^+$ T Cells Promote Experimental Cerebral Malaria by Modulating CD8$^+$ T Cell Accumulation within the Brain

Ana Villegas-Mendez, Rachel Greig, Tovah N. Shaw, J. Brian de Souza, Emily Gwyer Findlay, Jason S. Stumhofer, Julius C. R. Hafalla, Daniel G. Blount, Christopher A. Hunter, Eleanor M. Riley and Kevin N. Couper

J Immunol 2012; 189:968-979; Prepublished online 20 June 2012;
doi: 10.4049/jimmunol.1200688
http://www.jimmunol.org/content/189/2/968

The Journal of Immunology is published twice each month by
The American Association of Immunologists, Inc.,
1451 Rockville Pike, Suite 650, Rockville, MD 20852

Print ISSN: 0022-1767 Online ISSN: 1550-6606.

IFN-γ–Producing CD4$^+$ T Cells Promote Experimental Cerebral Malaria by Modulating CD8$^+$ T Cell Accumulation within the Brain

Ana Villegas-Mendez,*[,1,2] Rachel Greig,*[,1,3] Tovah N. Shaw,*[,2] J. Brian de Souza,*[,†] Emily Gwyer Findlay,*[,4] Jason S. Stumhofer,[‡,5] Julius C. R. Hafalla,* Daniel G. Blount,*[,6] Christopher A. Hunter,[‡] Eleanor M. Riley,* and Kevin N. Couper*

It is well established that IFN-γ is required for the development of experimental cerebral malaria (ECM) during *Plasmodium berghei* ANKA infection of C57BL/6 mice. However, the temporal and tissue-specific cellular sources of IFN-γ during *P. berghei* ANKA infection have not been investigated, and it is not known whether IFN-γ production by a single cell type in isolation can induce cerebral pathology. In this study, using IFN-γ reporter mice, we show that NK cells dominate the IFN-γ response during the early stages of infection in the brain, but not in the spleen, before being replaced by CD4$^+$ and CD8$^+$ T cells. Importantly, we demonstrate that IFN-γ–producing CD4$^+$ T cells, but not innate or CD8$^+$ T cells, can promote the development of ECM in normally resistant IFN-γ$^{-/-}$ mice infected with *P. berghei* ANKA. Adoptively transferred wild-type CD4$^+$ T cells accumulate within the spleen, lung, and brain of IFN-γ$^{-/-}$ mice and induce ECM through active IFN-γ secretion, which increases the accumulation of endogenous IFN-γ$^{-/-}$ CD8$^+$ T cells within the brain. Depletion of endogenous IFN-γ$^{-/-}$ CD8$^+$ T cells abrogates the ability of wild-type CD4$^+$ T cells to promote ECM. Finally, we show that IFN-γ production, specifically by CD4$^+$ T cells, is sufficient to induce expression of CXCL9 and CXCL10 within the brain, providing a mechanistic basis for the enhanced CD8$^+$ T cell accumulation. To our knowledge, these observations demonstrate, for the first time, the importance of and pathways by which IFN-γ–producing CD4$^+$ T cells promote the development of ECM during *P. berghei* ANKA infection. *The Journal of Immunology*, 2012, 189: 968–979.

Plasmodium berghei ANKA infection in susceptible strains of mice results in the development of experimental cerebral malaria (ECM), a fatal neuropathology characterized by the sequestration of parasite-infected RBCs (pRBC) and leukocytes within the brain (reviewed in Refs. 1–3). The clinical signs of ECM, including ataxia, paralysis, coma, and ultimately, death, are analogous to those of human cerebral malaria; as in human disease (reviewed in Ref. 1), although treatment with antimalarial drugs can prevent mortality associated with ECM, surviving mice may display long-lasting neurologic deficits, including impaired memory (4, 5).

IFN-γ–dependent processes are involved in the development of cerebral pathology during *P. berghei* ANKA infection, as evidenced by the complete resistance to ECM of IFN-γ$^{-/-}$ and IFN-γR$^{-/-}$ mice on normally susceptible backgrounds (6, 7). IFN-signaling pathways are significantly upregulated within the brains of ECM-susceptible mice during infection with *P. berghei* ANKA, suggesting that IFN-γ may directly influence the local cerebral environment (8, 9). In support of this hypothesis, IFN-γ was shown to promote macrophage accumulation and macrophage effector functions in the brain during infection (6), as well as to direct migration of CD8$^+$ T cells into the brain through CXCL9- and CXCL10-dependent pathways (7, 10-13). Although the functional role of brain-accumulating macrophages/monocytes in promoting ECM is unclear (14, 15), it is well established that T cells contribute to the initiation and/or terminal development of cerebral pathology (1, 3, 14). IFN-γ also promotes the upregulation of adhesion molecules on brain endothelial cells during infection, potentially enhancing pRBC and leukocyte sequestration within the brain vasculature and transmigration of cells into the perivascular space. (6, 10). Indeed, it was recently shown that pRBC and leukocyte accumulation is reduced in the brains of IFN-γ$^{-/-}$ mice during infection (15, 16).

IFN-γ can be produced by various cell populations during malaria infection, including NK cells, NKT cells, γδ TCR$^+$ T cells, and αβ TCR$^+$ CD4$^+$ and CD8$^+$ T cells (reviewed in Refs. 17, 18). Strikingly, and consistent with the notion of temporal activation of innate and adaptive immune responses, sequential production

*Department of Immunology and Infection, Faculty of Infectious and Tropical Diseases, London School of Hygiene and Tropical Medicine, London WC1E 7HT, United Kingdom; †Department of Immunology and Molecular Pathology, University College London Medical School, London W1T 4JF, United Kingdom; and ‡Department of Pathobiology, University of Pennsylvania, Philadelphia, PA 19104

[1]A.V.-M. and R.G. contributed equally to this work.

[2]Current address: Faculty of Life Sciences, University of Manchester, Manchester, U.K.

[3]Current address: Breakthrough Breast Cancer, London, U.K.

[4]Current address: Medical Research Council Centre for Inflammation Research, Queen's Medical Research Institute, University of Edinburgh, Edinburgh, U.K.

[5]Current address: Department of Microbiology and Immunology, University of Arkansas for Medical Sciences, Little Rock, AR.

[6]Current address: Oxford BioMedica Ltd., Oxford, U.K.

Received for publication February 29, 2012. Accepted for publication May 9, 2012.

This work was supported by the Wellcome Trust (074538) and the Biotechnology and Biological Sciences Research Council (BBSRC) (Grants 004161 and 020950) and by a Medical Research Council Career Development Award (Grant G0900487 to K.N.C.). R.G. was supported by a BBSRC doctoral training award.

Address correspondence and reprint requests to Dr. Kevin N. Couper at the current address: University of Manchester, Faculty of Life Sciences, AV Hill Building, Oxford Road, Manchester M13 9PT, U.K. E-mail address: kevin.couper@manchester.ac.uk

The online version of this article contains supplemental material.

Abbreviations used in this article: EAE, experimental autoimmune encephalomyelitis; ECM, experimental cerebral malaria; eYFP, enhanced yellow fluorescent protein; MFI, mean fluorescence intensity; p.i., postinfection; pRBC, parasite-infected RBC; WT, wild-type.

of IFN-γ by NK cells and $CD4^+$ T cells was shown to occur in vitro following exposure of PBMCs to *Plasmodium falciparum* parasites (19). In some malaria infections, IFN-γ production by $CD4^+$ T cells may be transient as a result of changes in the immunological environment. For example, during *P. chabaudi* AS and *P. yoelii* infections, changes in the dendritic cell compartment in the later stages of infection result in reduced IFN-γ production by $CD4^+$ T cells concomitant with upregulation of IL-4 and IL-10 production (20, 21). With specific relevance to *P. berghei* infection, an early burst of IFN-γ during the early stages of infection was associated with protection against ECM (22). Although there are many potential cellular sources of IFN-γ during *P. berghei* ANKA infection, it is unclear whether IFN-γ production by an individual cell population in a specific tissue location governs the development of ECM or whether sequential or concomitant induction of IFN-γ by different cell types and in different locations is required.

Although ECM is referred to as a classical IFN-γ–mediated condition, it was shown that IFN-γ–producing $CD4^+$ T cells are essential for the migration and recruitment of Th17 cells into the CNS during experimental autoimmune encephalomyelitis (EAE) (23) and that Th17 cells, rather than IFN-γ–producing cells, are responsible for much of the pathology of EAE (24, 25). Thus, it is possible that IL-17 mediates the development of ECM during *P. berghei* ANKA infection downstream of IFN-γ production. IL-17 can exert a number of direct effects in the CNS that may contribute to neuropathology during malaria infection, including direct neuronal damage (26), disruption of the blood–brain barrier (27), and activation of astrocytes (28, 29). The role of IL-17 during *P. berghei* ANKA infection has not been examined in detail.

In this study, we ruled out any role for IL-17 in the development of ECM and used IFN-γ reporter mice (30) to examine the dynamics of IFN-γ production within distinct anatomical locations during *P. berghei* ANKA infection. We subsequently calculated the contribution of IFN-γ production by each distinct cell type to the total IFN-γ response. Despite the myriad of cells that can produce IFN-γ during infection, using an adoptive-transfer model, we show that IFN-γ production specifically by $CD4^+$ T cells, and not by innate cells or $CD8^+$ T cells, can promote signs of ECM in normally resistant infected IFN-$\gamma^{-/-}$ mice. Finally, we provide mechanistic evidence that IFN-γ production exclusively by $CD4^+$ T cells causes ECM by increasing $CD8^+$ T cell migration and accumulation within the brain, potentially via the local upregulation of CXCL9 and CXCL10 within the brain. Our results significantly extend our understanding of the pathogenesis of ECM during *P. berghei* ANKA infection.

Materials and Methods

Animals and parasites

C57BL/6N (wild-type [WT]), C57BL/6 IFN-γ knockout (IFN-$\gamma^{-/-}$), C57BL/6 RAG-1 knockout (RAG-$1^{-/-}$), and C57BL/6 Ly5.1 (Ly5.1^+) mice were bred in-house at London School of Hygiene and Tropical Medicine or purchased from Harlan (Oxford, U.K.). C57BL/6 IFN-γ reporter mice (YETI: 30) were kindly provided by Dr. M. Mohrs (Trudeau Institute, Saranac Lake, NY) and were bred at Harlan. Animals were maintained in individual ventilated cages. C57BL/6 IL-17 receptor knockout (IL-17R$^{-/-}$) mice, provided by Amgen USA, which are deficient in IL-17A and IL-17F responses, were bred and maintained in the Department of Pathobiology, University of Pennsylvania. C57BL/6J mice used as controls in IL-17R$^{-/-}$ experiments were purchased from The Jackson Laboratory (Bar Harbor, ME) and were maintained at the University of Pennsylvania. Male and female mice were used in separate experiments between 6 and 10 wk of age.

Cryopreserved *P. berghei* ANKA parasites, derived from the *Pb*A clone 15cy1, were thawed and passaged once in vivo before being used to infect experimental animals. Experimental mice were infected i.v. with 10^4 parasitized RBCs. In some experiments, mice were injected i.p. with 250 μg anti-CD8 (53-7.62) or anti–IFN-γ (XMG1.2) on days −2, 0, 2, 4, and 6 of infection. Isotype control Abs (rat IgG2a and rat IgG1, respectively) were used to verify the specific activity of anti–IFN-γ and anti-CD8 mAbs administered in vivo. All Abs were obtained from BioXCell (West Lebanon, NH). Parasitemia was monitored daily by microscopic examination of Giemsa (BDH)-stained thin blood smears. Signs of disease were classified using the following clinical scale: 1 = no signs; 2 = ruffled fur/and or abnormal posture; 3 = lethargy; 4 = reduced responsiveness to stimulation and/or ataxia and/or respiratory distress/hyperventilation; and 5 = prostration and/or paralysis and/or convulsions. All animals were immediately euthanized when observed at stage 4 or 5. Stages 2 and 3 were classified as prodromal signs of ECM, and stages 4 and 5 were classified as ECM. Animals in stages 4 and 5 of infection invariably showed signs of cerebral pathology, including blocked vessels, hemorrhages, edema, perivascular cuffing and disruption, and damage to cerebral vasculature endothelial linings following histological examination.

Flow cytometry

Splenic single-cell suspensions were prepared by homogenization through a 70-μm cell strainer (BD Biosciences). Brains were chopped into small pieces and incubated in HBSS containing 10% FCS with collagenase/dispase (final concentration 2 mg/ml) (Sigma-Aldrich, Gillingham, U.K.) for 45 min at room temperature. The suspension was filtered through a 70-μm cell strainer before being overlaid on a 30% Percoll gradient and centrifuged at 1800 × *g* for 10 min. The pellet was collected, and the supernatant was discarded. Spleen and brain samples were treated with RBC lysing buffer (BD Pharmingen) to remove RBCs, washed, and resuspended in flow cytometry buffer (HBSS with 2% FCS). Absolute cell numbers were calculated using a hemocytometer, and live/dead cell differentiation was performed using trypan blue (Sigma-Aldrich). To examine T cell activation, 1×10^6 cells/sample were surface stained with anti-mouse CD4 (RM4.4), anti-mouse CD8 (53-6.7), anti-mouse CD44 (IM7), anti-mouse CD62L (MEL-14), anti-mouse CD69 (H1.2F3), anti-mouse CD71 (R17217), anti-mouse CD27 (LG.7F9), anti-mouse KLRG-1 (2F1), anti-mouse CD25 (PC61), anti-mouse CCR5 (HM-CCR5), anti-mouse CXCR3 (CXCR3-173), and anti-mouse CD45.1 (A20) or permeabilized (0.1% saponin/PBS) and stained with anti-mouse granzyme B (NGZB). NK and NKT cells were identified by staining with anti-mouse CD3 (145-2C11) and anti-mouse CD49b (DX5). To assess intracellular cytokine production, 1×10^6 live cells were incubated with PMA (200 ng/ml) and ionomycin (1 μg/ml) in the presence of brefeldin A (1:1000) for 5 h at 37˚C, 5% CO_2. The cells were washed and stained after permeabilizing cells with anti-mouse IFN-γ (XMG1.2) and anti-mouse TNF (MP6-XT22). All Abs were obtained from eBioscience or BD Biosciences. Fluorescence minus one controls and isotype-control Abs were used to validate flow cytometric results. Flow cytometric acquisition was performed using a FACSCalibur (BD Immunocytometry Systems), LSR II (BD Immunocytometry Systems), or Miltenyi MACSQuant (Miltenyi Biotec), and all analyses were performed using FlowJo software (TreeStar, Ashland, OR).

Determination of cerebral pathology

To examine the status (permeability) of the blood–brain barrier, mice were injected i.v. with 200 μl 1% Evans blue (Sigma-Aldrich). After 1 h, mice were sacrificed, and the brains were removed following whole-body perfusion with 15 ml PBS. In separate experiments, brains were removed from mice (following perfusion) that were not injected with Evans blue and placed in 10% formol saline. Preserved samples were then sectioned and stained with H&E (Independent Histopathology Services, London, U.K.). The presence of hemorrhages, inflamed and damaged blood vessels (including occluded vessels), and perivascular cuffing was examined by microscopy.

Real-time PCR

RNA isolation from brains was performed using RNeasy isolation kits, according to the manufacturer's instructions (QIAGEN). Isolated RNA was treated with DNAse to remove genomic DNA prior to synthesis of cDNA. cDNA expression for each sample was standardized using the housekeeping gene β-actin. Validated TaqMan gene-expression assays for β-actin, CXCL9, CXCL10, VCAM-1, and ICAM-1 were purchased from ABI Biosystems (Warrington, U.K.). PCR cycling (TaqMan, ABI 7500 fast RT-PCR) conditions were 50˚C for 2 min, 95˚C for 10 min followed by 40 cycles of 15 s at 95˚C, completed with 1 min at 60˚C. Parasite levels were determined by SYBR Green PCR using *P. berghei* 18s and *P. berghei* carbamoyl phosphate synthetase DNA primers, normalized to mouse β-actin or tyrosine 3-monooxygenase activation protein (YWHAZ), respectively. *P. berghei* 18s primers: 5′-AAGCATTAAATAAAGCGAATACATCCTTAC-3′ and 5′-GGAGATTGGTTTTGACGTTTATGTG-3′; β-actin primers:

5′-GTGGGCCGCTCTAGGCACCAA-3′ and 5′-CTCTTTGATGTCACGCACGATTTC-3′; carbamoyl phosphate synthetase primers 5′-TGGAATGTGTGAACATGATAAATA-3′ and 5′-TTTCCTGGCCCATTTGATAA-3′; YWHAZ primers: 5′-TTCTATTCCTCTATTTCCATGTTGG-3′ and 5′-AGGAGGAGGAGGAAGAGGAG-3′. All PCR data are presented as fold change (log_{10}) in gene expression in brains from infected IFN-$\gamma^{-/-}$ mice that received adoptively transferred $CD4^+$ T cells or infected control IFN-$\gamma^{-/-}$ mice that did not receive $CD4^+$ T cells relative to levels in brains from naive mice. Results for each gene were calculated using the Equation $2^{\wedge(\text{average normalized naive} - \text{normalized sample})}$.

Adoptive transfers

Splenic single-cell suspensions were prepared from naive WT or RAG-$1^{-/-}$ mice, as described above. In separate experiments, 40×10^6 WT splenocytes or 5×10^6 RAG-$1^{-/-}$ splenocytes (providing equivalent numbers of NK cells) were adoptively transferred into recipient mice by i.v. injection on the day before (−1) or on day 5 of *P. berghei* ANKA infection. Splenic $CD4^+$ and $CD8^+$ T lymphocytes were positively selected using anti-mouse–conjugated MidiMACS beads, according to the manufacturer's instructions (Miltenyi Biotec). A total of $5–10 \times 10^6$ purified T cell populations was adoptively transferred, depending on the experiment, into recipient mice by i.v. injection on the day before (−1) or on day 5 of *P. berghei* ANKA infection. The purity and phenotype of positively selected T cell populations were assessed by flow cytometry prior to adoptive transfer and were typically found to be >90%. $CD4^+$ and $CD8^+$ T cells were ~95% TCR $\alpha\beta^+$ and $CD3^+$. Representative plots showing the purity and heterogeneous activation status of donor $CD4^+$ T cells based upon CD44, CD62L, CD71, CD27, CXCR3, and CCR5 expression were provided for review during submission.

Statistical analysis

The normality of all data was tested using the D'Agostino and Pearson omnibus normality test. For comparisons between two groups, statistical significance was determined using either the *t* test or the Mann–Whitney *U* test, depending on normality of the data. For comparisons among three or more groups, statistical significance was determined using a one-way ANOVA, with the Tukey post hoc analysis for normally distributed data, or a Kruskal–Wallis test, with Dunn post hoc analysis for nonparametric data. All statistical analyses were performed using GraphPad Prism. In all cases, results were classified as significantly different when $p < 0.05$.

Results

IL-17 does not contribute to ECM during P. berghei *ANKA infection*

To assess the roles of IL-17 and IFN-γ in the development of ECM, we infected IFN-$\gamma^{-/-}$ mice, IL-17R$^{-/-}$ mice, and WT control mice with *P. berghei* ANKA and monitored various parameters of infection (Fig. 1). In accordance with previous observations (14, 31), all WT mice developed ECM and succumbed to infection by day 9 postinfection (p.i.), with a parasitemia < 35% (Fig. 1A, 1B). ECM was defined as a clinical score of 4 or 5 using the grading system described in *Materials and Methods*. In addition, WT mice showed substantial weight loss from day 7 p.i. (Fig. 1C). Importantly, the course of *P. berghei* ANKA infection in IL-17R$^{-/-}$ mice, which are deficient in IL-17A and IL-17F responses, was indistinguishable from that observed in WT mice, with similar parasite burdens (except on day 9 p.i., when a greater parasitemia was observed in IL-17R$^{-/-}$ mice) and weight loss throughout the course of infection (Fig. 1A–C). All IL-17R$^{-/-}$ mice succumbed to infection by day 9 p.i.; upon histological examination, similar numbers of comparably sized hemorrhages were observed in the brains of IL-17R$^{-/-}$ and WT mice (Fig. 1D). Furthermore, leukocyte and pRBC accumulation was observed in cerebral blood vessels of both WT and IL-17R$^{-/-}$ mice (Fig. 1D). In contrast, IFN-$\gamma^{-/-}$ mice were protected from the development of ECM and survived to day 27 p.i. before succumbing to hyperparasitemia and severe anemia (Fig. 1A, 1C, data not shown). Consistent with previous findings (7), minimal inflammation was observed in brains of IFN-$\gamma^{-/-}$ mice, which were removed at the time when WT and IL-17R$^{-/-}$ mice developed ECM (Fig. 1D). Thus, these data confirm the essential role of IFN-γ and rule out a major role for IL-17 in the development of cerebral pathology during *P. berghei* ANKA infection.

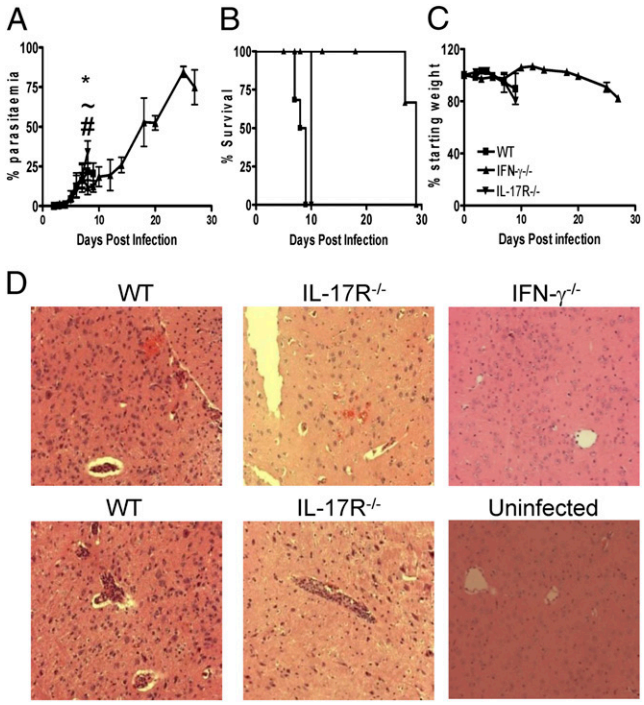

FIGURE 1. IFN-γ promotes ECM independently from IL-17. WT, IFN-$\gamma^{-/-}$, and IL-17R$^{-/-}$ mice were infected i.v. with 10^4 *P. berghei* ANKA pRBC. The course of infection was assessed by monitoring peripheral parasitemia (**A**), mortality (**B**), and weight loss (**C**). (**D**) Histological (H&E) staining of brain sections (cortex) demonstrating severity of cerebral pathology on day 8–9 of infection (original magnification ×20). The results are representative of two independent experiments (n = 3–5 mice/group). $^*p < 0.05$, WT versus IFN-$\gamma^{-/-}$ mice, $^{\sim}p < 0.05$, WT versus IL-17R$^{-/-}$ mice, $^{\#}p < 0.05$, IFN-$\gamma^{-/-}$ versus IL-17R$^{-/-}$ mice.

IFN-γ is produced by multiple leukocyte populations during P. berghei *ANKA infection*

IFN-γ is crucial for the development of ECM during *P. berghei* ANKA infection (6, 7, 32), but the cellular sources of IFN-γ are unclear. Thus, to investigate whether IFN-γ is produced by multiple cell types in a temporal or organ-specific manner or whether one cell type dominates the response, we examined the kinetics of IFN-γ mRNA transcription in IFN-γ reporter (YETI) mice on various days of infection. YETI mice developed ECM and succumbed to infection with comparable kinetics as did WT mice (Supplemental Fig. 1). Use of reporter mice overcame problems associated with low cell recovery from the brain during infection and the need for artificial mitogenic restimulation of cells ex vivo to measure cytokine production. Positive and negative enhanced yellow fluorescent protein (eYFP) gates were defined using non-eYFP WT mice (data not shown). Prior to infection, ~10–15% of splenic T cells, 20% of lung T cells, and 50% of brain-derived T cells expressed eYFP (Fig. 2A, 2B, data not shown); these cells were all $CD44^+$ high (results not shown) and are presumably polyclonal effector/memory T cells generated under homeostatic conditions (30). The higher frequency of eYFP expression in the brain compared with spleen or lung is consistent with the notion that only effector/memory T cells perform immune surveillance within the CNS (33, 34).

There were no consistent changes in the frequencies of eYFP$^+$ CD4$^+$ and CD8$^+$ T cells in the spleen or brain until day 7 of infection, at which point the frequencies of eYFP$^+$ CD4$^+$ and CD8$^+$ T cells increased in both organs (Fig. 2). Similarly, the mean fluorescence intensity (MFI) of eYFP expression (measuring the number of IFN-γ transcripts and consequently their capacity to produce IFN-γ) (35) by CD4$^+$ and CD8$^+$ T cells was highest on day 7 within both organs (Fig. 2D, 2G). Interestingly, in the brain, eYFP expression (MFI) was significantly higher by CD4$^+$ T cells compared with CD8$^+$ T cells on day 7 of infection, indicating that CD4$^+$ T cells were a greater source of IFN-γ on a cell-by-cell basis (Fig. 2G). Although the frequencies of splenic CD4$^+$eYFP$^+$ and CD8$^+$eYFP$^+$ T cells were similar throughout the course of infection, significantly greater absolute numbers of CD4$^+$eYFP$^+$ T cells were observed in the spleen at all time points compared with CD8$^+$eYFP$^+$ T cells (Fig. 2E). In contrast, higher numbers of CD8$^+$eYFP$^+$ T cells were observed in the brain on day 7 of infection (Fig. 2H). Numbers of eYFP$^+$CD4$^+$ and eYFP$^+$CD8$^+$ T cells were similar in all organs during the earlier stages of infection (Fig. 2E, 2H).

A high proportion (50–80%) of NK (CD3$^-$DX5$^+$) and NKT cells (CD3$^+$DX5$^+$) constitutively expressed eYFP in the spleen and brain of naive mice (Fig. 2A–C, 2F). Neither the frequencies of eYFP$^+$ NK cells nor the MFI of expression by NK cells changed significantly during the course of infection in any of the tissues, with the exception of a transient increase in MFI in the spleen on day 5 p.i. (Fig. 2D, 2G, data not shown). The frequencies of eYFP$^+$ NKT cells increased slightly on day 7 of infection in the spleen but not the brain (Fig. 2C, 2F), and the MFI of eYFP expression by NKT cells increased on days 5 and 7 in the spleen and on day 7 in the brain (Fig. 2D, 2G, data not shown). These results are consistent with

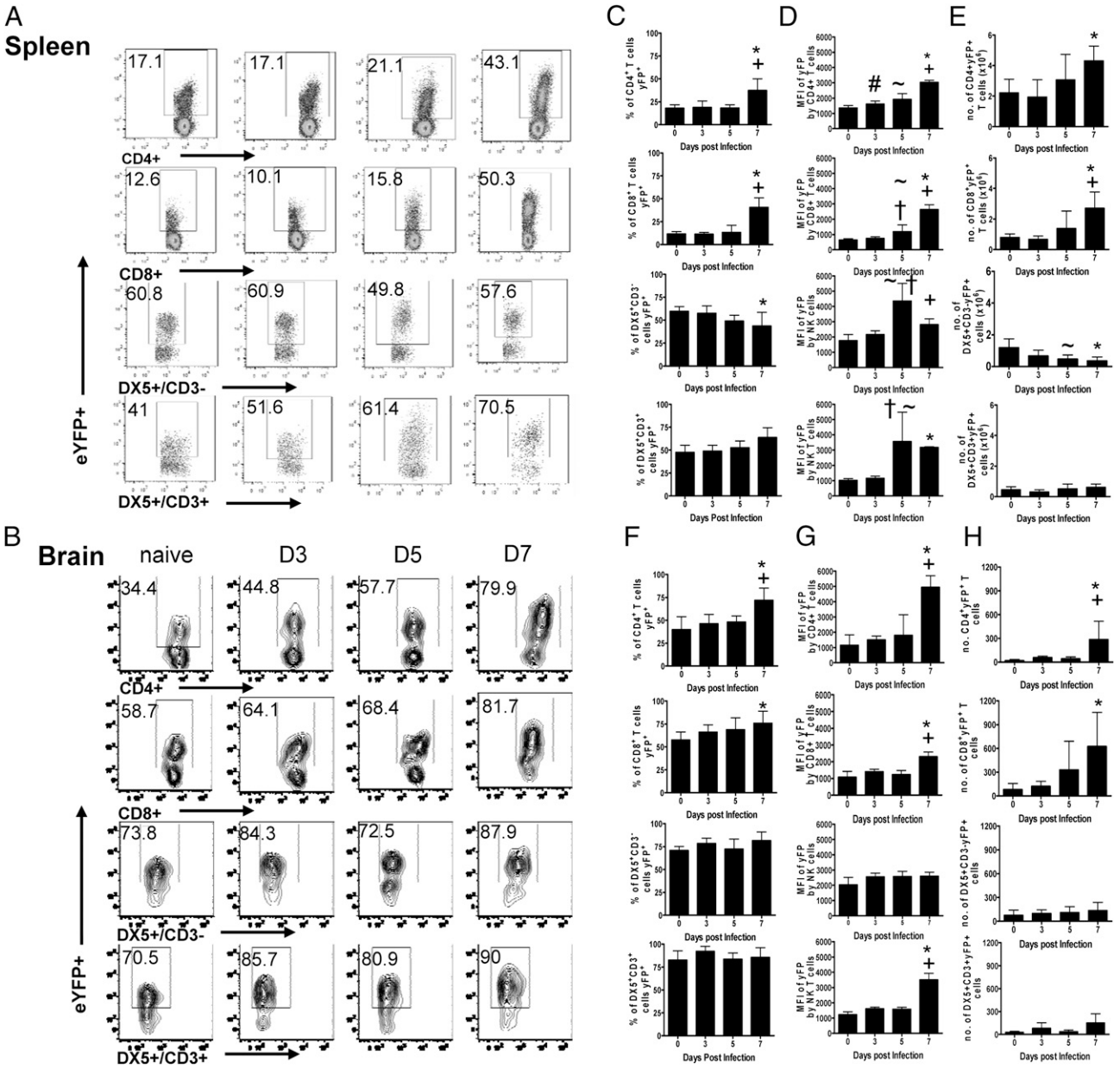

FIGURE 2. Multiple cell populations produce IFN-γ during *P. berghei* ANKA infection. IFN-γ eYFP reporter mice (YETI) were infected i.v. with 10^4 *P. berghei* ANKA pRBC. Representative plots showing eYFP expression by CD4$^+$, CD8$^+$ T cells, NK cells (CD3$^-$DX5$^+$), and NKT cells (CD3$^+$DX5$^+$) in the spleen (**A**) and brain (**B**) of naive mice and on days 3, 5, and 7 of infection. The frequencies (**C**, **F**), MFI (**D**, **G**), and total numbers (**E**, **H**) of IFN-γ–expressing cells within the spleen (C–E) and brain (F–H). The results are the mean ± SD of the group (n = 3–4 mice/group) and are representative of three separate experiments. $^{\#}p < 0.05$, D0 versus D3, $^{\sim}p < 0.05$, D0 versus D5, $^{*}p < 0.05$, D0 versus D7, $^{\dagger}p < 0.05$, D3 versus D5, $^{+}p < 0.05$, D5 versus D7.

previous reports showing that resting NK and NKT cells contain preformed IFN-γ mRNA and are poised for IFN-γ production (30). Nevertheless, the absolute numbers of splenic NK cells expressing eYFP did not change significantly in the brain, and declined significantly in the spleen, during infection (Fig. 2E, 2H). The absolute numbers of NKT cells expressing eYFP were low in comparison with the other populations and did not change significantly in any of the organs examined (Fig. 2E, 2H).

We next analyzed the total IFN-γ (eYFP) response within the spleen and brain during *P. berghei* ANKA infection to define the relative contribution of IFN-γ production from each cell type to the overall IFN-γ response (Fig. 3). $CD4^+$ T cells were found to be the dominant $eYFP^+$ population in the spleen throughout the course of infection, accounting for ~50% of all $eYFP^+$ cells. The NK cell contribution to the splenic eYFP response decreased significantly (from ~25% to <5%) during infection, being replaced principally by $CD8^+$ T cells. NKT cells and other cells represented ~12% of the total splenic $eYFP^+$ population throughout the course of infection (Fig. 3B). NK cells were the dominant population of $eYFP^+$ cells in the brain in naive mice but were rapidly outcompeted by $CD4^+$ and $CD8^+$ T cells during infection; $CD8^+$ T cells became the dominant $eYFP^+$ population in the brain (Fig. 3B). NKT cells and other cells represented ~15% of the $eYFP^+$ population in the brain (Fig. 3B). Combined, these data show that multiple cellular populations contribute to the IFN-γ response during infection, and the relative contribution of each population varies with stage of infection and tissue location.

IFN-γ–competent $\alpha\beta^+CD4^+$ T cells promote ECM in IFN-$\gamma^{-/-}$ recipient mice infected with P. berghei *ANKA*

Because several cell populations can produce IFN-γ during *P. berghei* ANKA infection, we established an adoptive-transfer model to examine which population(s) were the essential source(s) of IFN-γ leading to development of ECM. To demonstrate that it is possible to promote signs of ECM in IFN-$\gamma^{-/-}$ mice, we first adoptively transferred naive whole splenocytes from WT mice into IFN-$\gamma^{-/-}$ mice 1 d prior to infection. One hundred percent of IFN-$\gamma^{-/-}$ recipients of naive WT whole splenocytes developed prodromal signs of ECM (mean grade, 2.5, Table I), although none of the mice ultimately developed terminal cerebral complications. In contrast, adoptive transfer of naive splenocytes from RAG-$1^{-/-}$ mice into IFN-$\gamma^{-/-}$ mice failed to induce any signs of ECM (grade 1). Because these results suggested the importance of T cell sources of IFN-γ in the promotion of pathology, we next transferred αβ TCR^+ T cells purified from naive WT mice into IFN-$\gamma^{-/-}$ mice 1 d prior to infection with *P. berghei* ANKA. Importantly, adoptive transfer of naive WT TCR^+ T cells also promoted prodromal signs of ECM in 100% of IFN-$\gamma^{-/-}$ recipients (over three separate experiments), but the majority of animals did not progress to terminal ECM (mean grade, 3.1) (Table I). Interestingly, $CD4^+$ T cells appeared to be the most important source of pathogenic IFN-γ; adoptive transfer of naive $CD4^+$ T cells into IFN-$\gamma^{-/-}$ recipients 1 d before infection conferred partial susceptibility to infection, with animals showing some prodromal signs of ECM (mean grade, 2.8) (Table I), whereas adoptive transfer of naive $CD8^+$ T cells into IFN-$\gamma^{-/-}$ recipients 1 d before infection did not induce any signs of ECM (grade 1).

Taken together, the above data strongly indicated that $CD4^+$ T cells, and not $CD8^+$ T cells or innate cells, may be the most important source of pathogenic IFN-γ during *P. berghei* ANKA infection. However, because of the failure to induce terminal ECM in IFN-$\gamma^{-/-}$ mice following adoptive transfer of any population(s) of naive WT cells, we modified the model by adoptively transferring infection-derived WT leukocytes into IFN-$\gamma^{-/-}$ recipients. Based upon previous data showing that adoptive transfer of infection-derived WT $CD8^+$ T cells into naive $CXCR3^{-/-}$ mice immediately prior to infection promoted the development of fatal cerebral malaria (11, 12), we hypothesized that this approach may

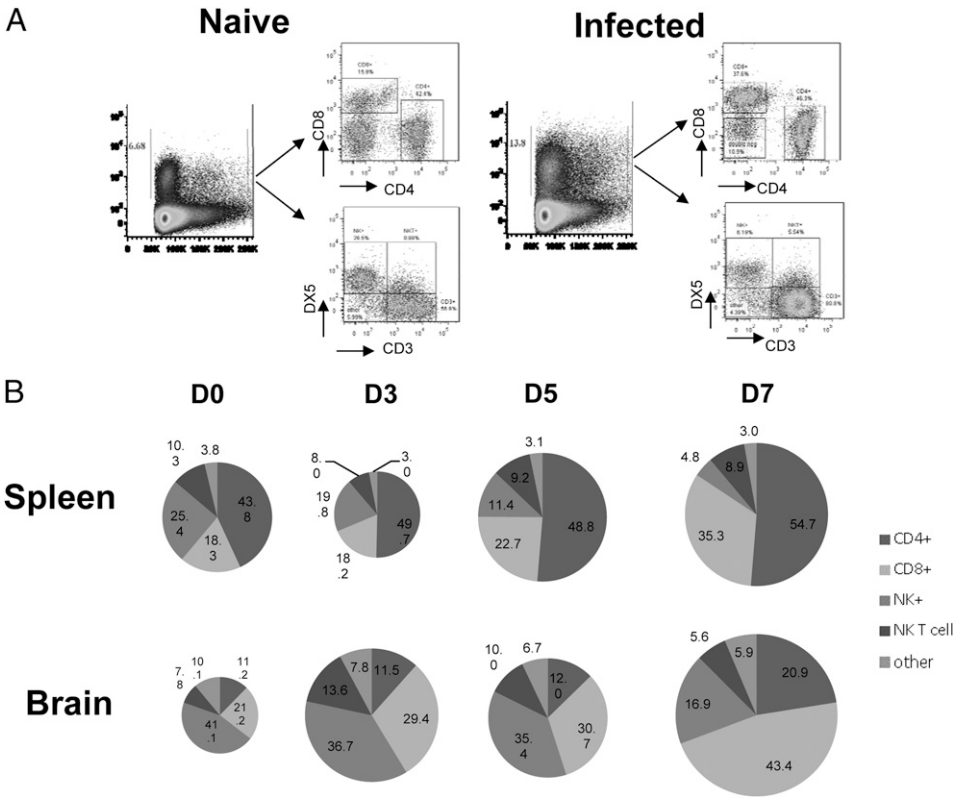

FIGURE 3. Temporal changes in cellular contribution to total IFN-γ response during infection. IFN-γ eYFP reporter mice (YETI) were infected i.v. with 10^4 *P. berghei* ANKA pRBC. (**A**) Representative plots showing the differentiation of cellular subsets within the total splenic eYFP response. (**B**) Pie charts showing the relative contribution of specific cellular populations to the total eYFP response in the spleen and brain in naive mice and on days 3, 5, and 7 of infection. The results are the mean of the group (n = 3–4 mice/group) and are representative of two separate experiments.

Table I. Incidence of ECM and severity of infection in IFN-$\gamma^{-/-}$ mice following adoptive transfer of naive and infection-derived IFN-γ–competent leukocytes

Population of Cells Transferred[a]	Day of Transfer	Incidence of Any Clinical Signs (%)[b]	Maximum Clinical Score (Mean)[b,c]	Incidence of Clinical Signs 4–5 (%)[b]	Total No. of Mice
Naive splenocytes	−1	100	2.5	0	8
Naive RAG-1$^{-/-}$ splenocytes	−1	0	1	0	6
Naive αβ$^+$ T cells	−1	100	3.1	9	11
Naive CD4$^+$ T cells	−1	100	2.8	0	8
Naive CD8$^+$ T cells	−1	0	1	0	8
I-D αβ$^+$ T cells	−1	100	3.25	25	8
I-D αβ$^+$ T cells	+5	100	3.75	50	8
I-D αβ$^+$ T cells	−1 and +5	100	≥4	100	10
I-D RAG-1$^{-/-}$ splenocytes	−1	0	1	0	6
I-D CD4$^+$ T cells	−1 and +5	100	4.6	100	17
I-D CD4$^+$ T cells	+5	100	3.0	0	7
I-D CD8$^+$ T cells	−1 and +5	0	1	0	14

All experiments were performed two to five times (n = 3–5 mice/group).
[a]WT C57/BL6 donors, unless stated otherwise.
[b]During ECM window period of infection (days 6–11).
[c]Grading system described in *Materials and Methods*.
I-D, Cells derived from infected (day 5) donors.

provide greater sensitivity to assess the ability of specific IFN-γ–producing cell populations to induce terminal ECM. Because our initial results suggested the importance of IFN-γ production by αβ TCR$^+$ T cells, we initially transferred WT αβ TCR$^+$ T cells (1:1 ratio of CD4$^+$/CD8$^+$ T cells), harvested from spleens of infected donor mice on day 5 of *P. berghei* ANKA infection (which represents the peak of T cell expansion and activation) (31), into IFN-$\gamma^{-/-}$ recipients on day −1 of infection. All recipient IFN-$\gamma^{-/-}$ mice developed prodromal signs of ECM (mean clinical grade, 3.25), but only 25% of mice that received cells on day −1 subsequently developed terminal ECM (Table I). As expected, adoptive transfer of infection-derived (day +5) RAG-1$^{-/-}$ splenocytes into IFN-$\gamma^{-/-}$ recipients on day −1 of infection did not promote any signs of disease (clinical grade 1). Notably, adoptive transfer of infection-derived (day +5) αβ TCR$^+$ T cells on day +5 of infection also promoted signs of disease in 100% of recipient mice (mean clinical grade, 3.75), and 50% of mice that received cells subsequently developed terminal ECM (Table I). Combined, these data indicated that IFN-γ production specifically by αβ TCR$^+$ T cells during the latter stages of infection (i.e., after day 5) can cause cerebral pathology, although our data do not rule out additional roles earlier in infection. In agreement with this dual-role hypothesis, adoptive transfer of infection-derived WT αβ TCR$^+$ T cells into IFN-$\gamma^{-/-}$ mice on days −1 and +5 of *P. berghei* ANKA infection induced late-stage ECM in all recipients (clinical grade ≥ 4), requiring all animals to be euthanized on day 6 or 7 (depending on the experiment) (Table I).

Using the same infection-derived adoptive-transfer system, we next examined whether IFN-γ–sufficient effector CD4$^+$ or CD8$^+$ T cell populations were individually able to promote ECM. Adoptive transfer of infection-derived (day +5) WT CD4$^+$ or CD8$^+$ T cell populations on days −1 and +5 did not affect peripheral parasitemia during the early stages of infection (Fig. 4A). Importantly, all IFN-$\gamma^{-/-}$ recipients of infection-derived WT CD4$^+$ T cells developed terminal ECM and were euthanized on day 6–7 p.i. (mean grade, 4.6), showing similar physical signs and brain pathology as infected WT mice, including cortical and cerebellar edema and hemorrhage (Fig. 4B–D, Table I, Table II). Adoptive transfer of infection-derived (day +5) CD4$^+$ T cells into IFN-$\gamma^{-/-}$ mice on day 5 of infection also caused prodromal signs of ECM (mean score, 3.0) (Table I). In contrast, and somewhat surprisingly, adoptive transfer of similar numbers of infection-derived WT CD8$^+$ T cells on days −1 and +5 did not induce cerebral pathology in IFN-$\gamma^{-/-}$ mice, and all recipients survived the acute phase of *P. berghei* ANKA infection (Fig. 4B, Table I). To our knowledge, these experiments are the first to demonstrate that

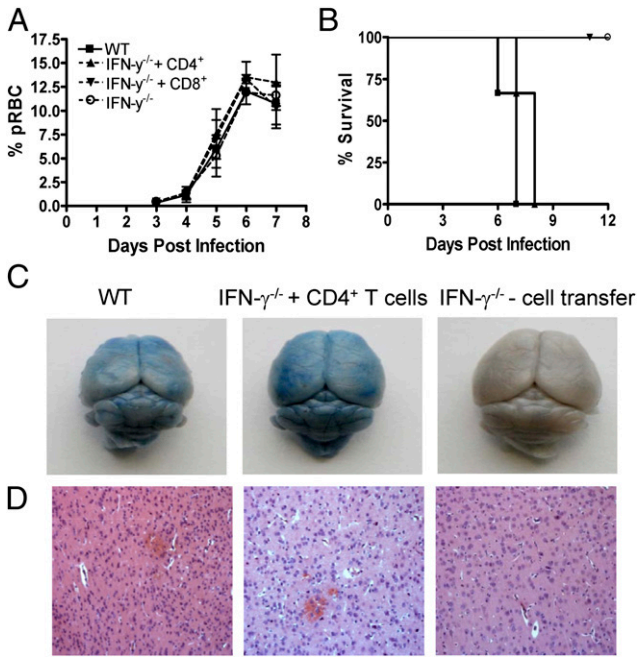

FIGURE 4. Infection-derived IFN-γ–competent CD4$^+$ T cells promote ECM in IFN-$\gamma^{-/-}$ mice infected with *P. berghei* ANKA. CD4$^+$ and CD8$^+$ T cells were purified from C57BL/6 mice on day 5 of *P. berghei* ANKA infection (10^4 pRBC i.v.) and were adoptively transferred (i.v.) separately into recipient IFN-$\gamma^{-/-}$ mice 1 d prior to infection with *P. berghei* ANKA (10^4 pRBC i.v.). A secondary adoptive transfer (i.v.) of day-5 infection-derived C57BL/6 CD4$^+$ or CD8$^+$ T cells into recipient IFN-$\gamma^{-/-}$ mice was performed on day 5 of infection. The course of infection was assessed by monitoring peripheral parasitemia (**A**) and mortality (**B**). The severity of cerebral pathology was determined on day 7 of infection by assessing the extravasation of Evans blue within the brain parenchyma (**C**) and histological (H&E) staining (original magnification ×20) (**D**). The results are the mean ± SD of the group (n = 3–4 mice/group) and are representative of five separate experiments.

Table II. Histological quantification of brain pathology

Group	Brain Petechial Hemorrhages/50 Fields[a]	Plugged Vessels/50 Fields[b]
WT	14 ± 7.3	30.6 ± 9.4
IFN-γ$^{-/-}$ + CD4$^+$ T cells[c]	12 ± 2.2	22 ± 4.5
IFN-γ$^{-/-}$	0.7 ± 1.2	6 ± 2.6

[a]H&E-stained brain transverse sections were examined, and the numbers of petechial hemorrhages in 50 fields were recorded. $p < 0.05$, WT versus IFN-γ$^{-/-}$, $p < 0.05$, IFN-γ$^{-/-}$ + CD4$^+$ T cells versus IFN-γ$^{-/-}$.

[b]H&E-stained brain transverse sections were examined, and the numbers of vessels plugged with leukocytes and/or pRBCs in 50 fields were recorded. $p < 0.05$, WT versus IFN-γ$^{-/-}$, $p < 0.05$, IFN-γ$^{-/-}$ + CD4$^+$ T cells versus IFN-γ$^{-/-}$.

[c]Infection-derived (day-5) CD4$^+$ T cells were transferred into IFN-γ$^{-/-}$ mice on days −1 and +5 of *P. berghei* ANKA infection.

IFN-γ production solely by CD4$^+$ T cells, and not by CD8$^+$ T cells or innate cells, can lead to the development of terminal ECM.

Adoptively transferred CD4$^+$ T cells migrate to lung and brain and promote ECM through active IFN-γ production

To define the mechanistic basis for the induction of ECM by WT CD4$^+$ T cells, we first determined the organ/tissue localization of adoptively transferred infection-derived CD4$^+$ T cells in recipient IFN-γ$^{-/-}$ mice. Donor Ly5.1$^+$ C57BL/6 CD4$^+$ T cells were clearly observed in the spleen, lung, and brain of recipient (Ly5.2$^+$) IFN-γ$^{-/-}$ mice on day 6 or 7 of infection (depending on experiment), when the recipient mice developed ECM (Fig. 5A, 5B). These adoptively transferred Ly5.1$^+$CD4$^+$ T cells maintained their ability to produce IFN-γ when restimulated in vitro (Fig. 5C, 5D). Importantly, neutralization of IFN-γ production in vivo by administration of anti–IFN-γ Ab (from days −2 to +6 of infection) completely blocked the ability of adoptively transferred CD4$^+$ T cells to induce ECM in IFN-γ$^{-/-}$ recipients (Fig. 5E). These data indicate that infection-derived WT CD4$^+$ T cells promote ECM in IFN-γ$^{-/-}$ mice by active secretion of IFN-γ, rather than through IFN-γ–independent effector functions imprinted during priming in an IFN-γ–sufficient (WT) environment.

Adoptive transfer of infection-derived CD4$^+$ T cells does not alter the host splenic T cell response

To determine whether adoptive transfer of infection-derived IFN-γ–competent CD4$^+$ T cells modified the host's endogenous splenic T cell response, which may have contributed to the development

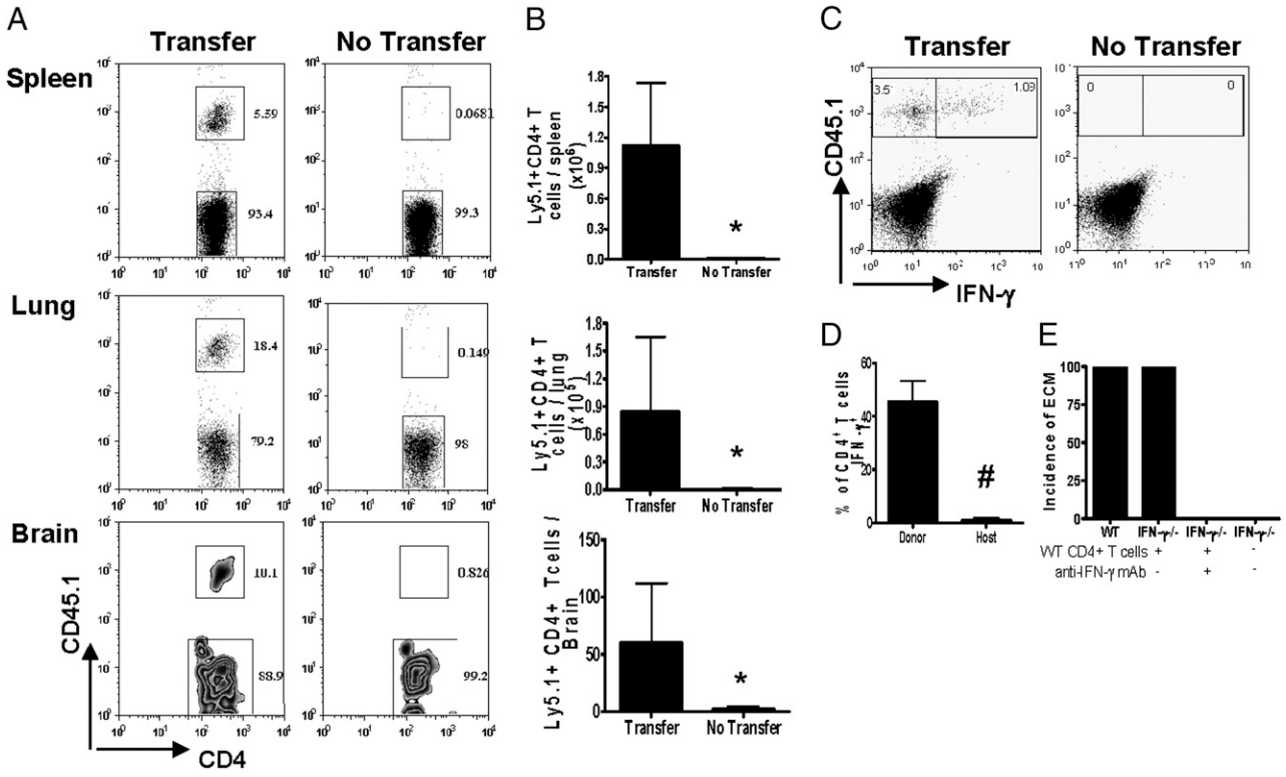

FIGURE 5. Adoptively transferred infection-derived IFN-γ–producing CD4$^+$ T cells accumulate in lymphoid and nonlymphoid tissues and induce ECM in IFN-γ$^{-/-}$ mice through active production of IFN-γ. CD4$^+$ T cells were purified from CD45.1$^+$C57BL/6 mice on day 5 of *P. berghei* ANKA infection (10^4 pRBC i.v.) and were adoptively transferred (i.v.) into recipient CD45.2$^+$IFN-γ$^{-/-}$ mice 1 d prior to infection with *P. berghei* ANKA (10^4 pRBC i.v.). A secondary adoptive transfer (i.v.) of day-5 infection-derived CD45.1$^+$C57BL/6 CD4$^+$ T cells into recipient IFN-γ$^{-/-}$ mice was performed on day 5 of infection. (**A**) Representative plots (gated on CD4$^+$ T cells) showing the recovery of host (CD45.1$^-$) and donor (CD45.1$^+$) CD4$^+$ T cells within the spleen, lung, and brain on day 7 of infection. (**B**) The numbers of recovered adoptively transferred cells within the spleen, lung, and brain. (**C**) Representative plots showing the production of IFN-γ by donor and host CD4$^+$ T cells within the spleen on day 7 of infection. (**D**) The frequency of donor and host CD4$^+$ T cells producing IFN-γ on day 7 of infection within the spleen. (**E**) The incidence of ECM in recipient and control IFN-γ$^{-/-}$ mice and recipient IFN-γ$^{-/-}$ mice treated with anti–IFN-γ Ab on days −2, 0, 2, 4, and 6. The results are the mean ± SD of the group (n = 3–4 mice/group) and are representative of two separate experiments. *$p < 0.05$, infected IFN-γ$^{-/-}$ recipients of WT cells versus infected IFN-γ$^{-/-}$ controls, $^{\#}p < 0.05$, donor CD4$^+$ T cells versus host CD4$^+$ T cells.

of ECM, we assessed the ability of endogenous splenic $CD4^+$ and $CD8^+$ T cells of IFN-$\gamma^{-/-}$ infected mice to produce TNF (Fig. 6). Although the role of TNF in promoting ECM in C57BL/6 mice during *P. berghei* ANKA infection has been questioned (36, 37), it is an informative measure of effector T cell proinflammatory functionality. Adoptive transfer of infection-derived WT ($CD45.1^+$) $CD4^+$ T cells did not significantly affect TNF production by host ($CD45.1^-$) splenic $CD4^+$ or $CD8^+$ T cells (Fig. 6A–C); indeed, host splenic $CD4^+$ T cells displayed an equivalent capacity to produce TNF during infection compared with adoptively transferred IFN-γ–competent $CD45.1^+CD4^+$ T cells (Fig. 6D).

In addition, the numbers of endogenous splenic $CD4^+$ and $CD8^+$ T cells were similar in IFN-$\gamma^{-/-}$ mice that did (transfer) or did not (no transfer) receive WT $CD4^+$ T cells (Fig. 6E, 6F); consistent with the lack of effect on TNF production, there were no significant differences in the frequencies of splenic $CD4^+$ or $CD8^+$ T cells that displayed an activated phenotype ($CD44^+$, $CD62L^{low}$, $CD69^+$, $CD71^+$, or GrB^+) (Fig. 6G–P). Together, these data demonstrate that IFN-γ–producing $CD4^+$ T cells cause ECM directly rather than by modulating the endogenous splenic T cell response. Although we previously showed that IFN-γ induces contraction of the splenic T cell response during *P. berghei* ANKA infection by promoting T cell apoptosis (31), adoptive transfer of IFN-γ–producing $CD4^+$ T cells did not reduce endogenous splenic T cell numbers (Fig. 6E, 6F), suggesting that the timing, concentration, location, or source of IFN-γ that drives the development of ECM may differ from the IFN-γ response that drives splenic T cell apoptosis.

IFN-γ–producing $CD4^+$ T cells promote ECM via $CD8^+$ T cell-dependent mechanisms

Because it is well established that $CD8^+$ T cell migration to and accumulation within the brain is required for the development of ECM in susceptible strains of mice (1, 3, 14), we hypothesized that transfer of infection-derived WT $CD4^+$ T cells would enhance the accumulation of host $CD8^+$ T cells in the brains of recipient IFN-$\gamma^{-/-}$ mice. As expected, significantly higher numbers of host $CD8^+$ T cells (but not host $CD4^+$ T cells) were observed in brains of IFN-$\gamma^{-/-}$ mice that received infection-derived IFN-γ–competent $CD4^+$ T cells than in brains of infected IFN-$\gamma^{-/-}$ mice that did not receive WT T cells (Fig. 7A, 7B). In addition, although adoptive transfer of WT $CD4^+$ T cells did not affect the frequencies of brain-accumulating host $CD8^+$ T cells that expressed CD44, adoptive transfer of WT $CD4^+$ T cells did significantly increase the frequencies of brain-accumulating host $CD8^+$ T cells that were $CD62L^{low}$, granzyme B^+, and KLRG-1^+, indicating that local $CD4^+$ T cell-derived IFN-γ may influence terminal differentiation and function of $CD8^+$ T cells in the brain (Fig. 7C–F). As expected, Ab-induced depletion of host $CD8^+$ T cells in IFN-$\gamma^{-/-}$ mice that had received WT effector $CD4^+$ T cells prevented the development of ECM (Fig. 7G–I): anti-CD8–treated mice remained healthy until the termination of the experiment on day 14. Together,

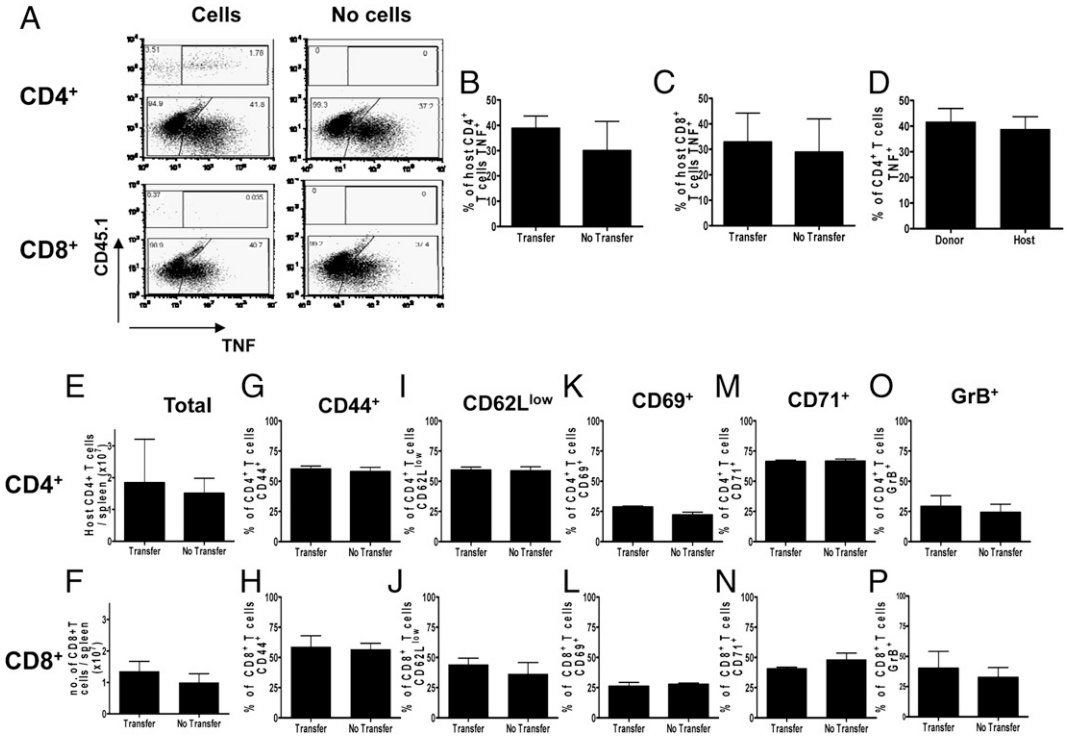

FIGURE 6. Adoptively transferred infection-derived IFN-γ–producing $CD4^+$ T cells do not alter host splenic $CD4^+$ or $CD8^+$ T cell responses in IFN-$\gamma^{-/-}$ mice during *P. berghei* ANKA infection. $CD4^+$ T cells were purified from $CD45.1^+$C57BL/6 mice on day 5 of *P. berghei* ANKA infection (10^4 pRBC i.v.) and were adoptively transferred (i.v.) into recipient $CD45.2^+$IFN-$\gamma^{-/-}$ mice 1 d prior to infection with *P. berghei* ANKA (10^4 pRBC i.v.). A secondary adoptive transfer (i.v.) of day-5 infection-derived $CD45.1^+$C57BL/6 $CD4^+$ T cells into recipient IFN-$\gamma^{-/-}$ mice was performed on day 5 of infection. (**A**) Representative plots showing the production of TNF by donor and host $CD4^+$ T cells and host $CD8^+$ T cells within the spleen on day 7 of infection. (**B**) Frequency of host splenic $CD4^+$ T cells producing TNF in adoptive transfer-recipient (Transfer) and control IFN-$\gamma^{-/-}$ mice (No Transfer) mice. (**C**) Frequency of host splenic $CD8^+$ T cells producing TNF in adoptive transfer-recipient (Transfer) and control IFN-$\gamma^{-/-}$ mice (No Transfer) mice. (**D**) Frequency of donor ($CD45.1^+$) and host ($CD45.1^-$) $CD4^+$ T cells producing TNF in the spleen of recipient IFN-$\gamma^{-/-}$ mice. The number of total host splenic $CD4^+$ (**E**) and $CD8^+$ (**F**) T cells. Frequencies of activated host splenic $CD4^+$ (**G**, **I**, **K**, **M**, **O**) and $CD8^+$ (**H**, **J**, **L**, **N**, **P**) T cells expressing $CD44^+$ (G, H), $CD62L^{low}$ (I, J), $CD69^+$ (K, L), $CD71^+$ (M, N), or GrB^+ (O, P) within the spleen of adoptive transfer-recipient (Transfer) and control IFN-$\gamma^{-/-}$ (No Transfer) mice. The results are the mean ± SD of the group (n = 3–4 mice/group) and are representative of three separate experiments.

these data show that IFN-γ–producing CD4+ T cells induce ECM in a CD8+ T cell-dependent manner but, crucially, the CD8+ T cells themselves do not need to be able to make IFN-γ.

IFN-γ–competent CD4+ T cells enhance the expression of proinflammatory chemokines in the brains of infected IFN-γ−/− mice

To determine the mechanism by which IFN-γ–competent, infection-derived CD4+ T cells mediate CD8+ T cell accumulation within the brains of IFN-γ−/− mice during *P. berghei* ANKA infection, we compared the expression of CXCL9, CXCL10, ICAM-1, and VCAM-1 mRNA in the brains of IFN-γ−/− mice that received infection-derived IFN-γ–competent CD4+ T cells relative to mRNA levels in control IFN-γ−/− mice that did not receive WT CD4+ T cells. At the time (day 6 or 7, depending on the experiment) when IFN-γ−/− mice that received WT CD4+ T cells developed ECM, significantly higher levels of CXCL9 and CXCL10 mRNA were detected in their brains than in brains of control IFN-γ−/− mice (Fig. 7J). In contrast, ICAM-1 and VCAM-1 expression was similar in the two groups of mice (Fig. 7J). Importantly, neutralization of IFN-γ significantly reduced the expression of CXCL9 and CXCL10 in the brain of IFN-γ−/− mice that received infection-derived IFN-γ–competent CD4+ T cells (Fig. 7J). To our knowledge, these results suggest, for the first time, that IFN-γ produced exclusively by CD4+ T cells is sufficient to modulate the cerebral environment, leading to the upregulated expression of key chemokines that control pathogenic CD8+ T cell accumulation in the brain (10–13).

IFN-γ–competent CD4+ T cells do not significantly increase brain parasite biomass

Adoptive transfer of infection-derived WT CD4+ T cells did not significantly alter the level of peripheral parasitemia in recipient IFN-γ−/− mice (Fig. 4A), suggesting that CD4+ T cells promoted ECM without significantly altering parasite burdens. Importantly, however, peripheral parasitemia does not necessarily reflect total tissue parasite biomass (38). Thus, we specifically examined whether adoptive transfer of IFN-γ–competent CD4+ T cells enhanced parasite sequestration/accumulation within the brain of IFN-γ−/− mice. Surprisingly, parasite gene expression (detecting *P. berghei* 18S and Carbamoyl phosphate synthetase genes) was not significantly increased in the brains of IFN-γ−/− mice that received IFN-γ–competent CD4+ T cells compared with the levels in the brains of IFN-γ−/− control-infected mice (Fig. 8). Moreover, we did not

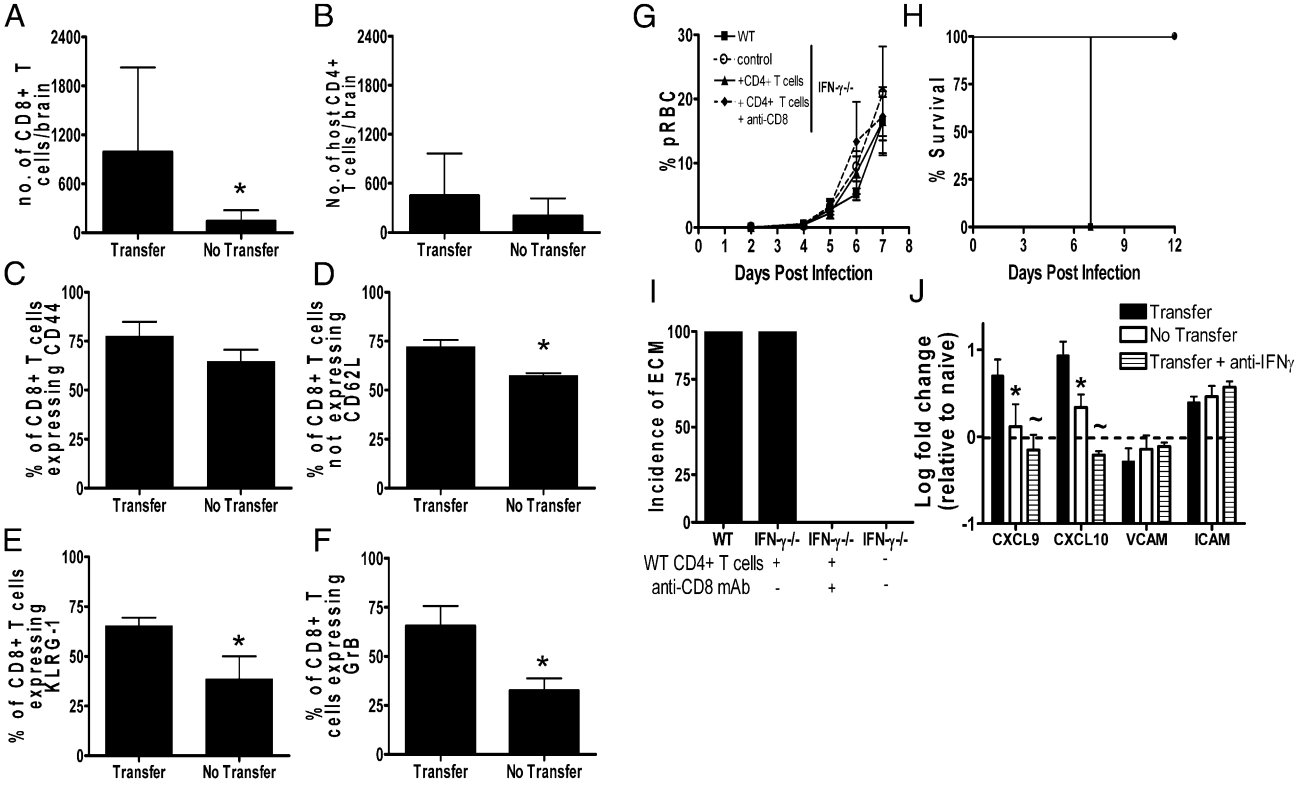

FIGURE 7. Adoptive transfer of infection-derived IFN-γ–producing CD4+ T cells promotes ECM in IFN-γ−/− mice by enhancing host CD8+ T cell responses within the brain. CD4+ T cells were purified from CD45.1+C57BL/6 mice on day 5 of *P. berghei* ANKA infection (10^4 pRBC i.v.) and were adoptively transferred (i.v.) into recipient CD45.2+IFN-γ−/− mice 1 d prior to infection with *P. berghei* ANKA (10^4 pRBC i.v.). A secondary adoptive transfer (i.v.) of day-5 infection-derived CD45.1+C57BL/6 CD4+ T cells into recipient IFN-γ−/− mice was performed on day 5 of infection. Number of host CD8+ T cells (**A**) and CD4+ T cells (**B**) within the brain. Frequencies of host CD8+ T cells in the brains of IFN-γ−/− mice that received IFN-γ–competent CD4+ T cells (Transfer) and control infected IFN-γ−/− mice (No Transfer) that were CD44+ (**C**), CD62L^{low} (**D**), KLRG-1+ (**E**), and GrB+ (**F**) on day 7 of infection. (**G**–**J**) Recipient mice were injected i.p. with 250 μg anti-CD8 on days −2, 0, 2, 4, and 6 of infection. Control recipients of CD4+ T cells were injected i.p. with PBS. The course of infection was monitored by following peripheral parasitemia (G) and survival (H). (I) The incidence of ECM was calculated. (J) The expression level of CXCL9, CXCL10, ICAM-1, and VCAM-1 in the brains of IFN-γ−/− mice that received WT CD4+ T cells compared with the level in infected IFN-γ−/− control mice that did not receive WT CD4+ T cells was calculated relative to the level of expression in naive brains by real-time PCR (TaqMan) on day 6 or 7 of infection, when the recipients of CD4+ T cells developed ECM. The results are the mean ± SD of the group (n = 3–4 mice/group) and are representative of two or three separate experiments. *$p < 0.05$, infected IFN-γ−/− recipients of WT cells versus infected IFN-γ−/− controls, ~$p < 0.05$, infected IFN-γ−/− recipients of WT cells versus infected IFN-γ−/− recipients of WT cells treated with anti–IFN-γ mAbs.

detect differences in total parasite biomass following adoptive transfer of infection-derived $CD4^+$ T cells using the well-established bioluminescence system (data not shown). Therefore, our results suggest that IFN-γ–producing $CD4^+$ T cells can induce ECM development without significantly altering the overall accumulation of parasites within the brain.

Discussion

ECM has historically been considered an IFN-γ–dependent immunopathological syndrome. However, the discovery of Th17 cells led to the reclassification of many conditions previously deemed to be Th1 dependent, including EAE and inflammatory arthritis (24, 25, 39). In this study, using IL-$17R^{-/-}$ mice that lack IL-17A and IL-17F responses (40), we found no evidence for a role for IL-17A or IL-17F in the development of cerebral pathology during *P. berghei* ANKA infection, which is consistent with a recent report demonstrating that IL-17A knockout mice are susceptible to ECM development (41). These results reaffirm the pivotal and IL-17–independent role of IFN-γ in the genesis of this condition. Indeed, we did not detect Th17 responses in WT or IFN-$\gamma^{-/-}$ mice at any point during infection (data not shown), indicating that—even in the absence of IFN-γ, which has been reported to block Th17 cell development (42)—*P. berghei* ANKA infection fails to generate an environment suitable for Th17 differentiation.

It is perhaps unsurprising that IFN-γ mRNA (as shown by eYFP) is expressed and/or upregulated by multiple cell populations during *P. berghei* ANKA infection. Nevertheless, our study demonstrates that the cell-specific contribution to the total eYFP response is governed by both the precise stage of infection and organ of location; some cell populations upregulate eYFP within tissues, whereas other $eYFP^+$ populations are lost. These data have important implications for not only understanding the protective and pathogenic function(s) of IFN-γ during infection but also for defining the tissue-specific signals required for the development and/or maintenance of IFN-γ–producing cell populations. Although upregulation of eYFP does not guarantee that a cell will go on to secrete IFN-γ (eYFP is a faithful marker of transcription but not translation), because *P. berghei* ANKA is an acute infection, covering only the early phases of T cell activation, it is highly probable that induction of eYFP in effector T cells reflects active protein translation (35). However, if NK cells and NKT cells are unable to rapidly translate constitutively expressed IFN-γ mRNA during infection (30), it is possible that their contribution to the overall IFN-γ response during infection may be overestimated in our analysis.

More importantly than dissecting the sources of IFN-γ during *P. berghei* ANKA infection, we demonstrated that IFN-γ produced solely by $CD4^+$ T cells is sufficient to promote the development of ECM. Although we acknowledge that we were only able to induce terminal ECM in IFN-$\gamma^{-/-}$ mice by adoptive transfer of infection-derived $CD4^+$ T cells, and not by adoptive transfer of naive $CD4^+$ T cells, we showed that infection-derived RAG-$1^{-/-}$ cells and infection-derived WT $CD8^+$ T cells are unable to promote any signs of ECM when adoptively transferred into IFN-$\gamma^{-/-}$ mice. Moreover, we showed that naive WT $CD4^+$ T cells, but not naive RAG-$1^{-/-}$ cells or naive WT $CD8^+$ T cells, promote comparable levels of disease as do whole naive splenocytes when adoptively transferred into IFN-$\gamma^{-/-}$ mice. Thus, when our naive and infection-derived adoptive transfer results are combined, our data very convincingly show that $CD4^+$ T cells are the predominant source of pathogenic IFN-γ during *P. berghei* ANKA infection. Although previous studies showed that $CD4^+$ T cells are involved in the development of ECM (7, 43-45), to our knowledge, this is the first definitive proof that they do so specifically through IFN-γ

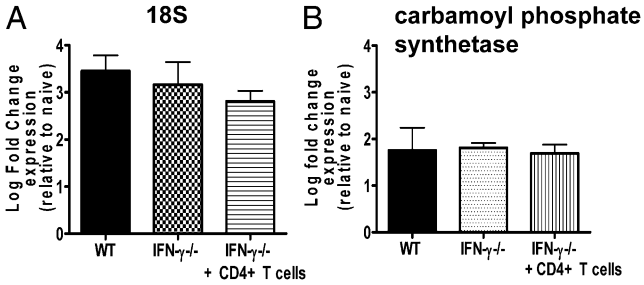

FIGURE 8. Adoptive transfer of infection-derived IFN-γ–producing $CD4^+$ T cells does not affect parasite accumulation within the brain during *P. berghei* ANKA infection. $CD4^+$ T cells were purified from C57BL/6 mice on day 5 of *P. berghei* ANKA infection (10^4 pRBC i.v.) and were adoptively transferred (i.v.) into recipient IFN-$\gamma^{-/-}$ mice 1 d prior to infection with *P. berghei* ANKA (10^4 pRBC i.v.). A secondary adoptive transfer (i.v.) of day-5 infection-derived C57BL/6 $CD4^+$ T cells into recipient IFN-$\gamma^{-/-}$ mice was performed on day 5 of infection. The expression levels of parasite 18S (**A**) and carbamoyl phosphate synthetase (**B**) genes in the perfused brains were determined on day 7 of infection by real-time PCR (SYBR Green). Results are expressed as the log fold change relative to the level in the brains of naive mice. The results are the mean ± SD of the group (n = 3–5 mice/group) and are representative of three separate experiments.

production. Our inability to induce ECM through naive cell transfers is potentially related to the specific immunological conditions induced during *P. berghei* ANKA infection, which possibly prevents the priming, maintenance, and survival of sufficient numbers of transferred cells in the recipient mice to cause ECM. Indeed, we and other groups have previously described the proapoptotic environment induced by *P. berghei* ANKA infection (31, 46), which causes the contraction of the T cell effector response.

$CD4^+$ T cells, rather than $CD8^+$ T cells, may be the most important source of IFN-γ during *P. berghei* ANKA infection, simply because—in the brain, at least—they produce much more IFN-γ on a per-cell basis than do $CD8^+$ T cells. But it is also possible that $CD4^+$ and $CD8^+$ T cells accumulate in different anatomical locations within the brain (e.g., in the subarachnoid space or perivascular spaces, where localized IFN-γ production is more, or less, damaging). Crucially, however, we showed that IFN-γ–producing $CD4^+$ T cells cannot, by themselves, induce ECM in IFN-$\gamma^{-/-}$ mice; adoptive transfer of IFN-γ–producing $CD4^+$ T cells into infected IFN-$\gamma^{-/-}$ mice increased endogenous $CD8^+$ T cell accumulation within the brain, and depletion of endogenous $CD8^+$ T cells prevented the onset of ECM. Thus, our data indicate that IFN-γ–producing $CD4^+$ T cells drive the development of ECM during *P. berghei* ANKA infection by facilitating the entry and accumulation of $CD8^+$ T cells into the brain, which then mediate pathology through IFN-γ–independent mechanisms.

Although it was recently shown that $CD4^+$ T cells are required for the activation of pathogenic $CD8^+$ T cells during *P. berghei* ANKA infection (45), we do not believe that IFN-γ–producing $CD4^+$ T cells simply activate $CD8^+$ T cells in the lymphoid compartment or periphery during infection, allowing their migration to the CNS, because transfer of WT infection-derived $CD8^+$ T cells (which were primed in the presence of IFN-γ–sufficient $CD4^+$ T cells) was not sufficient to induce ECM. While it is possible that IFN-γ–producing $CD4^+$ T cells directly modulate $CD8^+$ T cell effector function after day 5 of infection, when the $CD8^+$ T cells were purified for adoptive transfer, we do not believe this to be likely because the activation and effector functions of splenic $CD8^+$ T cells are seemingly unimpaired in IFN-$\gamma^{-/-}$ mice on day 7 of infection, when WT mice develop ECM (31). These data, when taken together with our finding in this study that adoptive

transfer of WT CD4+ T cells into infected IFN-γ$^{-/-}$ mice leads to upregulation of the chemokines CXCL9 and CXCL10 within the brain, lead us to conclude that the major role of IFN-γ–secreting CD4+ T cells, which accumulate in the brain through IFN-γ–independent mechanisms (31), is to modulate the localized brain environment, facilitating the migration/accumulation of CD8+ T cells into the brain. This hypothesis is consistent with upregulation of genes associated with IFN signaling in the brains of ECM-susceptible mice infected with *P. berghei* ANKA (8, 9) and with studies showing much lower expression of CXCL9 and CXCL10 in brains of ECM-resistant IFN-γ$^{-/-}$ mice than in brains of susceptible WT mice during *P. berghei* ANKA infection (7, 10, 31). The CD8+ T cell effector mechanisms responsible for progression to end-stage ECM are poorly understood; the data presented in this article indicate that CD8+ T cells do not need to produce IFN-γ, which is in agreement with a very recent study indicating that CD8+ T cells do not need to express IFN-γ for their accumulation or pathogenic function within the brain (47); however, evidence from other studies indicates a role for granzyme B-dependent and perforin-mediated killing of brain endothelial cells (47–49).

We also showed that adoptive transfer of IFN-γ–producing CD4+ T cells does not affect total parasite transcript levels within the brain of IFN-γ$^{-/-}$ mice during *P. berghei* ANKA infection. We also failed to detect differences in parasite biomass with the bioluminescence system, as used by Amante et al. (16) and Claser et al. (15) (data not shown but provided to reviewers during manuscript review). These results are surprising, because a number of recent studies showed that IFN-γ–dependent parasite accumulation in the brain is a key feature of ECM and is necessary for the development of pathology (15, 16, 49-51). However, there is some debate on the precise role of CD4+ T cells in mediating parasite accumulation within tissues during *P. berghei* ANKA infection; Amante et al. (16) recently suggested that CD4+ T cells are required for parasite accumulation within tissues, whereas Claser et al. (15) reported that CD4+ T cells do not facilitate parasite accumulation within the brain. Nonetheless, our results suggest that, in our ECM model, extensive parasite accumulation within the brain is not essential for the development of cerebral pathology, which may underline the heterogeneity of the ECM syndrome. However, although adoptive transfer of CD4+ T cells did not significantly increase total parasite levels within the brain, increased accumulation within specific and small regions of the brain would not necessarily have been detected in our analysis. In this scenario, parasite accumulation within a small number of specific and focal regions may have been sufficient to cause ECM. Crucially, we do not yet understand the precise regions of the brain that are most sensitive to parasite accumulation and inflammation during malaria infection, leading to death (52). Identifying whether (and how) *P. berghei* ANKA parasites sequester within the brain microvessels and the relative importance of this process for the development of ECM are ongoing areas of research in our and other laboratories.

In summary, we have examined the cellular sources of IFN-γ during *P. berghei* ANKA infection and, to our knowledge, highlighted for the first time that CD4+ T cells promote the development of ECM specifically through their production of IFN-γ. Our results suggest that IFN-γ produced by CD4+ T cells may act locally within the brain to modify the brain environment, which is required for the accumulation of CD8+ T cells within the brain, leading to ECM. These data represent a significant advancement in our understanding of the pathogenesis of ECM during *P. berghei* ANKA infection, which may have implications for understanding, and, therefore, either preventing or treating, human cerebral malaria.

Acknowledgments

We thank Dr. Chris Engwerda and Dr. Ash Haque (Queensland Institute of Medical Research, Brisbane, QLD, Australia) for discussion and critical reading of the manuscript.

Disclosures

The authors have no financial conflicts of interest.

References

1. de Souza, J. B., J. C. Hafalla, E. M. Riley, and K. N. Couper. 2010. Cerebral malaria: why experimental murine models are required to understand the pathogenesis of disease. *Parasitology* 137: 755–772.
2. Riley, E. M., K. N. Couper, H. Helmby, J. C. Hafalla, J. B. de Souza, J. Langhorne, W. B. Jarra, and F. Zavala. 2010. Neuropathogenesis of human and murine malaria. *Trends Parasitol.* 26: 277–278.
3. Good, M. F., H. Xu, M. Wykes, and C. R. Engwerda. 2005. Development and regulation of cell-mediated immune responses to the blood stages of malaria: implications for vaccine research. *Annu. Rev. Immunol.* 23: 69–99.
4. Dai, M., S. E. Reznik, D. C. Spray, L. M. Weiss, H. B. Tanowitz, M. Gulinello, and M. S. Desruisseaux. 2010. Persistent cognitive and motor deficits after successful antimalarial treatment in murine cerebral malaria. *Microbes Infect.* 12: 1198–1207.
5. Reis, P. A., C. M. Comim, F. Hermani, B. Silva, T. Barichello, A. C. Portella, F. C. Gomes, I. M. Sab, V. S. Frutuoso, M. F. Oliveira, et al. 2010. Cognitive dysfunction is sustained after rescue therapy in experimental cerebral malaria, and is reduced by additive antioxidant therapy. *PLoS Pathog.* 6: e1000963.
6. Amani, V., A. M. Vigário, E. Belnoue, M. Marussig, L. Fonseca, D. Mazier, and L. Rénia. 2000. Involvement of IFN-gamma receptor-medicated signaling in pathology and anti-malarial immunity induced by *Plasmodium berghei* infection. *Eur. J. Immunol.* 30: 1646–1655.
7. Belnoue, E., S. M. Potter, D. S. Rosa, M. Mauduit, A. C. Grüner, M. Kayibanda, A. J. Mitchell, N. H. Hunt, and L. Rénia. 2008. Control of pathogenic CD8+ T cell migration to the brain by IFN-gamma during experimental cerebral malaria. *Parasite Immunol.* 30: 544–553.
8. Miu, J., N. H. Hunt, and H. J. Ball. 2008. Predominance of interferon-related responses in the brain during murine malaria, as identified by microarray analysis. *Infect. Immun.* 76: 1812–1824.
9. Lovegrove, F. E., S. A. Gharib, S. N. Patel, C. A. Hawkes, K. C. Kain, and W. C. Liles. 2007. Expression microarray analysis implicates apoptosis and interferon-responsive mechanisms in susceptibility to experimental cerebral malaria. *Am. J. Pathol.* 171: 1894–1903.
10. Van den Steen, P. E., K. Deroost, I. Van Aelst, N. Geurts, E. Martens, S. Struyf, C. Q. Nie, D. S. Hansen, P. Matthys, J. Van Damme, and G. Opdenakker. 2008. CXCR3 determines strain susceptibility to murine cerebral malaria by mediating T lymphocyte migration toward IFN-gamma-induced chemokines. *Eur. J. Immunol.* 38: 1082–1095.
11. Miu, J., A. J. Mitchell, M. Müller, S. L. Carter, P. M. Manders, J. A. McQuillan, B. M. Saunders, H. J. Ball, B. Lu, I. L. Campbell, and N. H. Hunt. 2008. Chemokine gene expression during fatal murine cerebral malaria and protection due to CXCR3 deficiency. *J. Immunol.* 180: 1217–1230.
12. Campanella, G. S., A. M. Tager, J. K. El Khoury, S. Y. Thomas, T. A. Abrazinski, L. A. Manice, R. A. Colvin, and A. D. Luster. 2008. Chemokine receptor CXCR3 and its ligands CXCL9 and CXCL10 are required for the development of murine cerebral malaria. *Proc. Natl. Acad. Sci. USA* 105: 4814–4819.
13. Nie, C. Q., N. J. Bernard, M. U. Norman, F. H. Amante, R. J. Lundie, B. S. Crabb, W. R. Heath, C. R. Engwerda, M. J. Hickey, L. Schofield, and D. S. Hansen. 2009. IP-10-mediated T cell homing promotes cerebral inflammation over splenic immunity to malaria infection. *PLoS Pathog.* 5: e1000369.
14. Belnoue, E., M. Kayibanda, A. M. Vigario, J. C. Deschemin, N. van Rooijen, M. Viguier, G. Snounou, and L. Rénia. 2002. On the pathogenic role of brain-sequestered alphabeta CD8+ T cells in experimental cerebral malaria. *J. Immunol.* 169: 6369–6375.
15. Claser, C., B. Malleret, S. Y. Gun, A. Y. Wong, Z. W. Chang, P. Teo, P. C. See, S. W. Howland, F. Ginhoux, and L. Rénia. 2011. CD8+ T cells and IFN-γ mediate the time-dependent accumulation of infected red blood cells in deep organs during experimental cerebral malaria. *PLoS ONE* 6: e18720.
16. Amante, F. H., A. Haque, A. C. Stanley, Fde. L. Rivera, L. M. Randall, Y. A. Wilson, G. Yeo, C. Pieper, B. S. Crabb, T. F. de Koning-Ward, et al. 2010. Immune-mediated mechanisms of parasite tissue sequestration during experimental cerebral malaria. *J. Immunol.* 185: 3632–3642.
17. McCall, M. B., and R. W. Sauerwein. 2010. Interferon-γ–central mediator of protective immune responses against the pre-erythrocytic and blood stage of malaria. *J. Leukoc. Biol.* 88: 1131–1143.
18. Schroder, K., P. J. Hertzog, T. Ravasi, and D. A. Hume. 2004. Interferon-gamma: an overview of signals, mechanisms and functions. *J. Leukoc. Biol.* 75: 163–189.
19. Horowitz, A., K. C. Newman, J. H. Evans, D. S. Korbel, D. M. Davis, and E. M. Riley. 2010. Cross-talk between T cells and NK cells generates rapid effector responses to *Plasmodium falciparum*-infected erythrocytes. *J. Immunol.* 184: 6043–6052.
20. Perry, J. A., C. S. Olver, R. C. Burnett, and A. C. Avery. 2005. Cutting edge: the acquisition of TLR tolerance during malaria infection impacts T cell activation. *J. Immunol.* 174: 5921–5925.

21. Sponaas, A. M., E. T. Cadman, C. Voisine, V. Harrison, A. Boonstra, A. O'Garra, and J. Langhorne. 2006. Malaria infection changes the ability of splenic dendritic cell populations to stimulate antigen-specific T cells. *J. Exp. Med.* 203: 1427–1433.
22. Mitchell, A. J., A. M. Hansen, L. Hee, H. J. Ball, S. M. Potter, J. C. Walker, and N. H. Hunt. 2005. Early cytokine production is associated with protection from murine cerebral malaria. *Infect. Immun.* 73: 5645–5653.
23. O'Connor, R. A., C. T. Prendergast, C. A. Sabatos, C. W. Lau, M. D. Leech, D. C. Wraith, and S. M. Anderton. 2008. Cutting edge: Th1 cells facilitate the entry of Th17 cells to the central nervous system during experimental autoimmune encephalomyelitis. *J. Immunol.* 181: 3750–3754.
24. Veldhoen, M., R. J. Hocking, R. A. Flavell, and B. Stockinger. 2006. Signals mediated by transforming growth factor-beta initiate autoimmune encephalomyelitis, but chronic inflammation is needed to sustain disease. *Nat. Immunol.* 7: 1151–1156.
25. Bettelli, E., Y. Carrier, W. Gao, T. Korn, T. B. Strom, M. Oukka, H. L. Weiner, and V. K. Kuchroo. 2006. Reciprocal developmental pathways for the generation of pathogenic effector TH17 and regulatory T cells. *Nature* 441: 235–238.
26. Siffrin, V., H. Radbruch, R. Glumm, R. Niesner, M. Paterka, J. Herz, T. Leuenberger, S. M. Lehmann, S. Luenstedt, J. L. Rinnenthal, et al. 2010. In vivo imaging of partially reversible th17 cell-induced neuronal dysfunction in the course of encephalomyelitis. *Immunity* 33: 424–436.
27. Kebir, H., K. Kreymborg, I. Ifergan, A. Dodelet-Devillers, R. Cayrol, M. Bernard, F. Giuliani, N. Arbour, B. Becher, and A. Prat. 2007. Human TH17 lymphocytes promote blood-brain barrier disruption and central nervous system inflammation. *Nat. Med.* 13: 1173–1175.
28. Das Sarma, J., B. Ciric, R. Marek, S. Sadhukhan, M. L. Caruso, J. Shafagh, D. C. Fitzgerald, K. S. Shindler, and A. Rostami. 2009. Functional interleukin-17 receptor A is expressed in central nervous system glia and upregulated in experimental autoimmune encephalomyelitis. *J. Neuroinflammation* 6: 14.
29. Ma, X., S. L. Reynolds, B. J. Baker, X. Li, E. N. Benveniste, and H. Qin. 2010. IL-17 enhancement of the IL-6 signaling cascade in astrocytes. *J. Immunol.* 184: 4898–4906.
30. Stetson, D. B., M. Mohrs, R. L. Reinhardt, J. L. Baron, Z. E. Wang, L. Gapin, M. Kronenberg, and R. M. Locksley. 2003. Constitutive cytokine mRNAs mark natural killer (NK) and NK T cells poised for rapid effector function. *J. Exp. Med.* 198: 1069–1076.
31. Villegas-Mendez, A., J. B. de Souza, L. Murungi, J. C. Hafalla, T. N. Shaw, R. Greig, E. M. Riley, and K. N. Couper. 2011. Heterogeneous and tissue-specific regulation of effector T cell responses by IFN-gamma during *Plasmodium berghei* ANKA infection. *J. Immunol.* 187: 2885–2897.
32. Grau, G. E., H. Heremans, P. F. Piguet, P. Pointaire, P. H. Lambert, A. Billiau, and P. Vassalli. 1989. Monoclonal antibody against interferon gamma can prevent experimental cerebral malaria and its associated overproduction of tumor necrosis factor. *Proc. Natl. Acad. Sci. USA* 86: 5572–5574.
33. Kwok, L. Y., H. Miletic, S. Lütjen, S. Soltek, M. Deckert, and D. Schlüter. 2002. Protective immunosurveillance of the central nervous system by *Listeria*-specific CD4 and CD8 T cells in systemic listeriosis in the absence of intracerebral *Listeria*. *J. Immunol.* 169: 2010–2019.
34. Wilson, E. H., W. Weninger, and C. A. Hunter. 2010. Trafficking of immune cells in the central nervous system. *J. Clin. Invest.* 120: 1368–1379.
35. Mayer, K. D., K. Mohrs, S. R. Crowe, L. L. Johnson, P. Rhyne, D. L. Woodland, and M. Mohrs. 2005. The functional heterogeneity of type 1 effector T cells in response to infection is related to the potential for IFN-gamma production. *J. Immunol.* 174: 7732–7739.
36. Grau, G. E., L. F. Fajardo, P. F. Piguet, B. Allet, P. H. Lambert, and P. Vassalli. 1987. Tumor necrosis factor (cachectin) as an essential mediator in murine cerebral malaria. *Science* 237: 1210–1212.
37. Engwerda, C. R., T. L. Mynott, S. Sawhney, J. B. De Souza, Q. D. Bickle, and P. M. Kaye. 2002. Locally up-regulated lymphotoxin alpha, not systemic tumor necrosis factor alpha, is the principle mediator of murine cerebral malaria. *J. Exp. Med.* 195: 1371–1377.
38. Franke-Fayard, B., J. Fonager, A. Braks, S. M. Khan, and C. J. Janse. 2010. Sequestration and tissue accumulation of human malaria parasites: can we learn anything from rodent models of malaria? *PLoS Pathog.* 6: e1001032.
39. Toy, D., D. Kugler, M. Wolfson, T. Vanden Bos, J. Gurgel, J. Derry, J. Tocker, and J. Peschon. 2006. Cutting edge: interleukin 17 signals through a heteromeric receptor complex. *J. Immunol.* 177: 36–39.
40. Sarkar, S., L. A. Cooney, and D. A. Fox. 2010. The role of T helper type 17 cells in inflammatory arthritis. *Clin. Exp. Immunol.* 159: 225–237.
41. Ishida, H., C. Matsuzaki-Moriya, T. Imai, K. Yanagisawa, Y. Nojima, K. Suzue, M. Hirai, Y. Iwakura, A. Yoshimura, S. Hamano, et al. 2010. Development of experimental cerebral malaria is independent of IL-23 and IL-17. *Biochem. Biophys. Res. Commun.* 402: 790–795.
42. Harrington, L. E., R. D. Hatton, P. R. Mangan, H. Turner, T. L. Murphy, K. M. Murphy, and C. T. Weaver. 2005. Interleukin 17-producing CD4+ effector T cells develop via a lineage distinct from the T helper type 1 and 2 lineages. *Nat. Immunol.* 6: 1123–1132.
43. Grau, G. E., P. F. Piguet, H. D. Engers, J. A. Louis, P. Vassalli, and P. H. Lambert. 1986. L3T4+ T lymphocytes play a major role in the pathogenesis of murine cerebral malaria. *J. Immunol.* 137: 2348–2354.
44. Yañez, D. M., D. D. Manning, A. J. Cooley, W. P. Weidanz, and H. C. van der Heyde. 1996. Participation of lymphocyte subpopulations in the pathogenesis of experimental murine cerebral malaria. *J. Immunol.* 157: 1620–1624.
45. Haque, A., S. E. Best, A. Ammerdorffer, L. Desbarrieres, M. M. de Oca, F. H. Amante, F. de Labastida Rivera, P. Hertzog, G. M. Boyle, G. R. Hill, and C. R. Engwerda. 2011. Type I interferons suppress $CD4^+$ T cell-dependent parasite control during blood-stage *Plasmodium* infection. *Eur. J. Immunol.* 41: 2688–2698.
46. Hirunpetcharat, C., and M. F. Good. 1998. Deletion of *Plasmodium berghei*-specific CD4+ T cells adoptively transferred into recipient mice after challenge with homologous parasite. *Proc. Natl. Acad. Sci. USA* 95: 1715–1720.
47. Haque, A., S. E. Best, K. Unosson, F. H. Amante, F. de Labastida, N. M. Anstey, G. Karupiah, M. J. Smyth, W. R. Heath, and C. R. Engwerda. 2011. Granzyme B expression by CD8+ T cells is required for the development of experimental cerebral malaria. *J. Immunol.* 186: 6148–6156.
48. Potter, S., T. Chan-Ling, H. J. Ball, H. Mansour, A. Mitchell, L. Maluish, and N. H. Hunt. 2006. Perforin mediated apoptosis of cerebral microvascular endothelial cells during experimental cerebral malaria. *Int. J. Parasitol.* 36: 485–496.
49. Nitcheu, J., O. Bonduelle, C. Combadiere, M. Tefit, D. Seilhean, D. Mazier, and B. Combadiere. 2003. Perforin-dependent brain-infiltrating cytotoxic CD8+ T lymphocytes mediate experimental cerebral malaria pathogenesis. *J. Immunol.* 170: 2221–2228.
50. McQuillan, J. A., A. J. Mitchell, Y. F. Ho, V. Combes, H. J. Ball, J. Golenser, G. E. Grau, and N. H. Hunt. 2011. Coincident parasite and CD8 T cell sequestration is required for development of experimental cerebral malaria. *Int. J. Parasitol.* 41: 155–163.
51. Baptista, F. G., A. Pamplona, A. C. Pena, M. M. Mota, S. Pied, and A. M. Vigário. 2010. Accumulation of *Plasmodium berghei*-infected red blood cells in the brain is crucial for the development of cerebral malaria in mice. *Infect. Immun.* 78: 4033–4039.
52. Haldar, K., S. C. Murphy, D. A. Milner, and T. E. Taylor. 2007. Malaria: mechanisms of erythrocytic infection and pathological correlates of severe disease. *Annu. Rev. Pathol.* 2: 217–249.